Blind Image Quality Assessment Using a General Regression Neural Network

Chaofeng Li, *Member, IEEE*, Alan Conrad Bovik, *Fellow, IEEE*, and Xiaojun Wu

***Abstract*— We develop a no-reference image quality assessment (QA) algorithm that deploys a general regression neural network (GRNN). The new algorithm is trained on and successfully assesses image quality, relative to human subjectivity, across a range of distortion types. The features deployed for QA include the mean value of phase congruency image, the entropy of phase congruency image, the entropy of the distorted image, and the gradient of the distorted image. Image quality estimation is accomplished by approximating the functional relationship between these features and subjective mean opinion scores using a GRNN. Our experimental results show that the new method accords closely with human subjective judgment.**

***Index Terms*— Entropy, general regression neural network, gradient, image quality assessment, no-reference, phase congruency.**

I. Introduction

ALGORITHMS that automatically assess perceptual image quality are critical for numerous image processing applications. This problem is becoming increasingly important, owing to the near-ubiquitous presence of digital images in our daily lives. In recent years, considerable progress has been made on the problem of assessing quality relative to a presumed reference image [full-reference (FR) quality assessment (QA)], and a variety of successful FR objective image quality indices have been proposed that correlate well with human subjective judgment of quality [1]–[11]. The simplest and most widely used quality metrics are still the mean square error (MSE)—the averaging squared intensity differences of distorted and reference image pixels—and the scaled reciprocal of MSE, the peak signal-to-noise ratio (PSNR). However, the MSE and its variants do not correlate well with subjective quality measures [12]–[15]. Similarity index (MS-SSIM) [2] and its variants [9], the visual information fidelity index [10], and the visual several prominent FR objective metrics have been demonstrated to have much higher correlation with subjective judgment than the MSE, including the multi-scale structural signal-to-noise ratio [11]. However, these FR objective metrics require full access to the reference images.

Recently, the video quality experts group (VQEG) [16] has included RR image/video QA as one of its directions for future development. In RR algorithms [17]–[19], the reference image is not available, yet some features extracted from the reference image are made available. This is quite useful when the reference information must be transmitted with a low bandwidth. Yet, in many, and perhaps most possible applications, the availability of any reference information may be implausible. Examples include wireless videos received by cell phones and personal digital assistants, videos on the internet, images from commercial digital cameras, and so on. Quite often as least some of the distortions are unguessable in advance, as is the case, for example, with YouTube videos. A breakthrough in the development of generic full NR QA is highly desirable, although the true "blind" problem is often regarded as nearly unapproachable.

Yet human observers can easily judge the quality of distorted images without recourse to comparison with any reference image. Our still-limited understanding of both early and mid-stage processing in the visual cortical and extra-cortical regions increases this difficulty, as therefore the ultimate receiver of video is not well-understood. In the case where distortions are known, considerable progress has been made, and a variety of successful distortion-specific objective NR QAs have been proposed. For example, in [20] a natural scene statistics (NSS) model is used to define a blind measure of the quality of images compressed by JPEG 2000. In [21] an NR image QA (IQA) algorithm also targeting JPEG 2000 is advanced based on pixel distortions and edge information. Blind JPEG QA was considered in [22] using a spatial activity measure. In [23], a more specific (blur only) NR algorithm was developed also for JPEG 2000 images. In [24], a generic NSS-based NR QA algorithm operating in the discrete cosine transform (DCT) domain was proposed for JPEG or MPEG signals. Some algorithms do not target a specific compression algorithm, but rather a class of artifact. In [25], edge blocking is assessed by an NR algorithm operating on the fast Fourier transform. In [26], the cross-correlation of subsampled images is used to create a blockiness metric. In [27], the authors propose a metric based on computing gradients along block boundaries while tempering the result with a weighting function based on the human visual system. Other blind compression-specific QA algorithms were developed in [28] and [29], both based on block-based DCT coding.

Manuscript received June 22, 2010; revised November 26, 2010; accepted February 13, 2011. Date of publication April 12, 2011; date of current version May 4, 2011. This work was supported in part by the National Natural Science Foundation of China, under Grant 60973094, and the Fundamental Research Funds for the Central Universities, under Project JUSRP20915.

C. Li is with the Key Laboratory of Advanced Process Control for Light Industry (Ministry of Education), the School of IoT Engineering, Jiangnan University, Wuxi, Jiangsu 214122, China (e-mail: wxlichaofeng@126.com).

A. C. Bovik is with the Department of Electrical & Computer Engineering, University of Texas at Austin, Austin, TX 78712 USA (e-mail: bovik@ece.utexas.edu).

X. Wu is with the School of IoT Engineering, Jiangnan University, Wuxi, Jiangsu 214122, China (e-mail: wu_xiaojun@yahoo.com.cn).

Color versions of one or more of the figures in this paper are available online at http://ieeexplore.ieee.org.

Digital Object Identifier 10.1109/TNN.2011.2120620

Recently, several researchers have taken the approach to estimate the PSNR using the DCT or wavelet coefficients, then using the estimates for NR image or video QA [30]–[35]. Of course, since the PSNR itself is a poor objective image and video quality metric relative to human subjectivity [12], this approach is questionable.

Machine learning methods are powerful mathematical tools for solving nonlinear fitting or prediction problems. In particular, they can be used to construct good approximations of the functional relationships between known sets of input and output data. Several researchers have explored the possibility of using this capability to explore the relationship between reference and distorted images, viz, to predict image quality. In [36] and [37] a circular back propagation-based image quality method was proposed for evaluating the effects of image enhancement filters, using general pixel-based image features—such as higher order moments—but without considering perceptual factors. In [38], a growing and pruning radial basis function network was deployed to assess JPEG image artifacts using some loose perceptual features. In [39], a multilayer perception network was utilized to fuse three NR metrics into a single device for assessing the distortion in blurred images. In [40], the authors use singular vectors out of singular value decomposition as features for quantifying major structural information in images and then predict image quality by support vector regression.

In all the above mentioned NR QA methods, the algorithms developed are intended to assess only a single specific type of distortion (such as JPEG, JPEG2000, blur, or MPEG). Naturally, more general NR QA algorithms that are sensitive to multiple types of distortions are highly desired, since often, more than one type of distortion may exist in an image, and moreover, it may be unknown what type of distortion to expect. Recently, two NR QA algorithms for multiple types of distortions were reported. In [41], a new two-step framework called blind image quality index (BIQI) was presented for NR IQA based on NSS models. First, a classification algorithm is used to estimate the probabilities of a set of distortions being present in an image. Then, the severity (quality impact) of each distortion is assessed separately. The overall quality of the image is then expressed as a probability-weighted summation of the separate distortion-specific quality scores. The algorithm achieves a performance commensurate with PSNR when tested on the LIVE IQA Database [1]. In [42], another NR IQA algorithm called the BLIINDS index was proposed, which predicts image quality based on eight NSS features expressed as statistics of local DCT coefficients. The BLIINDS index also achieves performance close to the FR metric PSNR on the LIVE IQA Database [1]. However, both BIQI and BLIINDS have trouble handling two of the LIVE IQA Database distortions: JPEG and Fast Fading (FF) noise. The approach taken in this paper is complementary to these very recent approaches. Rather than deploying NSS-based features, the algorithm presented here utilizes perceptually relevant features to drive a GRNN-based NR QA algorithm able to handle multiple distortions.

This paper is organized as follows. Section II reviews related perceptual features, such as phase congruency, entropy and the image gradient. A new, GRNN-based IQA model is described in Section III. Section IV gives experimental results and discussion of the results. Finally, in Section V, we look toward future research on this difficult topic.

II. Relevant Perceptual Features

We utilize a number of image features that possess relevant information-bearing, perceptual content. These features are measurements of complementary aspects of the image content: phase congruency, local information and gradient. The first of these measures the degree of coherency of the local frequencies comprising the image; the second of these measures the available local information content of the image; while the third measures the perceptually relevant rate of change of image luminance. Any one of these loses relevance without the other two; phase congruence is less relevant where there is reduced image information and activity, i.e., less structure. The image information loses perceptual relevance when the local phase is erratic (random-like) and when the activity is low. The gradient is less important when the local information content is low, and there is little structure (phase congruency).

A. Phase Congruency

Phase congruency is a relatively new concept as an image feature. Image phase is an appealing quantity within the context of image quality or faithful representation, since it has been shown that much of perceptual information in an image signal is stored in the Fourier phase, rather than the Fourier amplitude [43], [44]. The underlying principle of phase congruency is that perceptually significant image features occur at spatial locations where the important Fourier components are maximally in-phase with one another [45].

Morrone and Owens [45] define the phase congruency function in terms of the Fourier series expansion of a signal I at a location x to be

$$PC_I(x) = \max_{\bar{\varphi}(x)\in[0,2\pi]} \frac{\sum_n A_n \cos[\varphi_n(x) - \bar{\varphi}(x)]}{\sum_n A_n} \quad (1)$$

where A_n is the amplitude of the nth Fourier component of I, $\phi_n(x)$ is the local phase of the Fourier component at x, and $\bar{\varphi}(x)$ is the average phase at x. The value of $\bar{\varphi}(x)$ that maximizes (1) is the amplitude weighted mean local phase angle of all the Fourier terms at coordinate x.

As it stands, phase congruency is a rather awkward quantity to calculate. As an alternative, points of maximum phase congruency can be calculated by searching for peaks in the local energy function, defined as [45]

$$E(x) = \sqrt{F^2(x) + H^2(x)} \quad (2)$$

where $F(x)$ is the signal $I(x)$ with its DC component removed, and $H(x)$ is the Hilbert transform of $F(x)$. Approximations to $F(x)$ and $H(x)$ can be found by convolving the signal with a quadrature pair of filters. Then it can be shown that phase congruency is equal to the ratio between the energy and the sum of the Fourier amplitudes [46]

$$PC_I(x) = \frac{E(x)}{\sum_n A_n}. \quad (3)$$

In (1), energy is proportional to the cosine of the weighted deviation of phase angle $\phi_n(x)$ from the mean phase. Although the cosine function is maximized when $\phi_n(x)$ becomes equal to the mean phase, a significant difference between $\phi_n(x)$ and the mean phase must occur before its value falls appreciably. Using the cosine of the phase deviation allows an insensitive measure of phase congruency [47].

Another measure of phase congruency that is easier to compute was developed in [47]

$$PC_{II}(x) = \frac{\sum_n W(x)\lfloor A_n(x)\Delta\phi_n(x) - T\rfloor}{\sum_n A_n(x) + \varepsilon} \tag{4}$$

where $\lfloor\rfloor$ is a floor function that leaves the argument unchanged if non-negative, and zero otherwise; $A_n(x) = \sqrt{e_n(x)^2 + o_n(x)^2}$ is the amplitude at a given wavelet scale, $[e_n(x), o_n(x)] = [I(x) * M_n^e, I(x) * M_n^o]$, I is the image signal, and M_n^e and M_n^o are the even-symmetric (cosine) and odd-symmetric (sine) wavelets at a scale n; $\Delta\phi_n(x) = \cos[\phi_n(x) - \bar{\phi}(x)] - |\sin[\phi_n(x) - \bar{\phi}(x)]|$ is a sensitive measure of phase deviation; $W(x) = 1/(1 + e^{r(c-s(x))})$ is a tapered weighting function, where $s(x) = (1/N)(\sum_n A_n(x)/A_{\max}(x) + \varepsilon)$, and where c is the cut-off value of filter response spread below which phase congruency values become penalized and γ is a gain factor that controls the sharpness of the cutoff; T is an estimate of the noise level (as detailed in [47]), and ε is a small constant that avoids division by zero.

Phase congruency appears to be perceptually relevant [48]. For example, Fig. 1 shows the "couple" image and the corresponding phase congruency image, which highlights many image regions that are of structural significance. Phase congruency has been applied to a variety of image processing problems, including compression and reconstruction [49], symmetry detection [50], segmentation [51], text recognition [52], [53], face recognition [54], [55], feature detection [47], [56], [57], and so on. In [58], the correlation between local phase coherence and the perception of blur was analyzed. However, phase congruency appears not to have been used to create image quality indices. In [59], the author used phase congruency to measure FR image similarity.

We believe that phase congruency is a relevant feature for blind IQA that does not require a comparison (reference) image. Phase distortions lead to significant perceptual image degradations, and can arise from many different distortion processes. Disruptions in the congruency of phase in an image may correlate well with perception of phase distortions. For computational reasons, we use the definition of phase congruency in (4). The MATLAB code for calculating phase congruency can be found at http://www.csse.uwa.edu.au/~pk/Research/MatlabFns/index.html.

B. Image Entropy

The sample entropy of the image I [60] is

$$E_I = -\sum_n p(n)\log_2 p(n) \tag{5}$$

where $p(n)$ denotes the empirical probability of luminance value n. Here, the MATLAB function entropy() will be used to compute the entropy of images. It has been used in a variety of ways, but only a few that are directly relevant to our application.

In [61], the entropy is used to identify the anisotropy of images. Following this, the authors of [62] deploy the entropy to measure the anisotropy of images, and use this statistic for blind IQA. The method appears to show promise, but was not extensively tested.

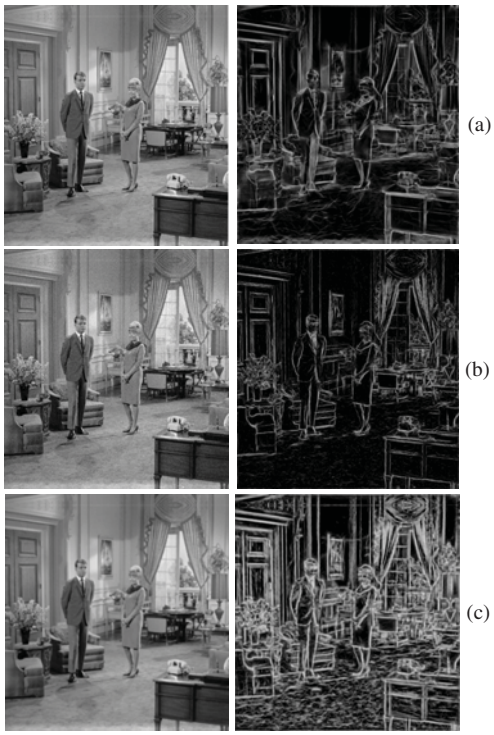

Fig. 1. Image "couple" and the associated phase congruency map. (a) Original image. (b) Noise contaminated image. (c) Blurred image.

1	2	1
0	0	0
−1	−2	−1

1	2	1
0	0	0
−1	−2	−1

Fig. 2. Sobel operator masks.

C. Image Gradient

The gradient $\nabla I = [\nabla I_x, \nabla I_y]$ is large when there are significant luminance variations in the image I, whether arising from discontinuous structures, from textured structures, or from random effects. A simple and robust measurement of the horizontal and vertical components of the gradient of I is generated by convolving I with the 3×3 Sobel operator masks shown in Fig. 2.

As usual, the gradient amplitude is estimated as the square root of the sum of the directional derivative estimates. For example, the mean value of the gradient amplitude of the Image "couple" in Fig. 1(a)–(c) is 71.93, 86.84, and 47.70, respectively.

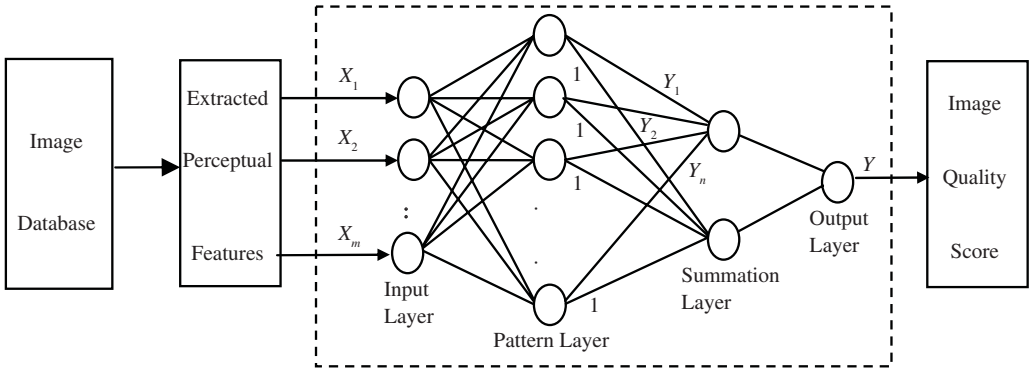

Fig. 3. Schematic diagram of GRNN for assessing image quality.

III. GRNN Image Quality Model

The general regression neural network (GRNN) is a powerful regression tool that has a dynamic network structure [63], [64]. It is based on established statistical principles, and asymptotically converges with an increasing number of samples to the optimal regression surface [65]. GRNN has been observed to yield better results than the back-propagation network or RBF network in terms of prediction performance [65], [66]. For an input vector X, the output $\overset{\Lambda}{Y}$ of the GRNN is [63]

$$\overset{\Lambda}{Y}(X) = \frac{\sum_{i=1}^{n} Y_i \exp(-D_i^2/2\sigma^2)}{\sum_{i=1}^{n} \exp(-D_i^2/2\sigma^2)} \tag{6}$$

where n is the number of sample observations; $D_i^2 = (X - X_i)^{\mathrm{T}}(X - X_i)$; X_i and Y_i are sample values; and σ is the spread parameter. The larger the value of σ, the smoother the functional approximation. In order to fit the data very closely, the selected value of the spread parameter should be smaller than the average distance between the input vectors.

A schematic diagram of the GRNN IQA architecture is shown in Fig. 3 (inside dashed box), which consists of four layers: the input layer, the pattern layer, the summation layer and the output layer. The number of inputs is equal to the number of independent features. Each unit in the pattern layer represents a training pattern. The summation layer includes two units: the first unit sums all the outputs of the pattern layer and assesses the numerator of (6), while the second unit assesses the denominator of (6). Each node in the pattern layer is connected to each of the two nodes in the summation layer. The weight on the connection between node i in the pattern layer and the first node of the summation layer is equal to Y_i. The weight of the connection between any node i in the pattern layer and the second node in the summation layer is equal to unity. The output unit computes the quotient of the two outputs of the summation layer, yielding the predicted value of the dependent feature.

IV. Experiments and Discussions

We selected the GRNN for the purpose of assessing image quality owing to its excellent prediction power. We use four perceptually motivated features as inputs to the GRNN, derived from those given in Section II: 1) the mean value of the phase congruency image of distorted image (MPC); 2) the entropy of the phase congruency image of distorted image (EPC); 3) the entropy of the distorted image (EDIS); and 4) the mean value of the gradient magnitude of the distorted image (MGDIS).

The GRNN was implemented using the MATLAB function *newgrnn*. The only parameter to be determined is the smoothness-of-fit parameter σ. Since there is no *a priori* method of selecting this parameter, we tried a variety of values in the range 0.01–0.1 for blind IQA.

A. Testing on LIVE Database

In our simulations we used the popular LIVE IQA Database [67]. This database includes five types of distorted images: JPEG, JPEG2000 (JP2K), White Noise (WN), Blur and FF. The database contains 29 different images and a total of 982 images (reference and distorted). In the following experiments, we remove all reference images from the database, and leave 779 images for training and testing. The database reflects the result of a large human study [1], and includes differential mean opinion scores (DMOS) for each distorted image.

Three performance measures are used to evaluate the algorithm. The first is the Spearman rank order correlation coefficient (SROCC) which measures the prediction monotonicity of the quality index. The second and third are the linear correlation coefficient (LCC) and the root MSE (RMSE) after non-linear regression. For the latter two measures, the logistic function specified in [68] was used to fit the model predictions to the subjective data.

The following procedure was used to test the new NR IQA algorithm. First, we divided the LIVE IQA Database into five datasets, each including six or five groups of images having identical content but different and varied levels of distortion, as shown in Table I. No content is shared between these smaller datasets. Cross validation was applied to these five datasets (each of the five datasets was used as the test set in turn, viz., 5-fold cross validation was used), yielding the results shown in Table II. We used the two recent NR IQA algorithms (BIQI [41] and BLIINDS [42] index) and two FR methods [PSNR and single-scale structural similarity (SS-SSIM)] for comparison. The spread parameter for fitting was set to 0.04.

TABLE I
IMAGE CATEGORIES FOR DIFFERENT DATA SETS

Data	Image Categories
Dataset 1	Bikes, house, paintedhouse, sailing1, statue, dancers
Dataset 2	Caps, cemetery, manfishing, lighthouse, sailing4, coinsinfountain
Dataset 3	Carnivaldolls, monarch, studentsculpture, ocean, parrots, sailing2
Dataset 4	Woman, flowersonih35, buildings, sailing3, stream, plane
Dataset 5	Churchandcapitol, lighthouse2, building2, womanhat, rapids

TABLE II
IQA RESULTS ON LIVE IQA DATABASE

Method		SROCC	LCC	RMS
GRNN	Dataset 1	0.8133	0.8274	8.9923
	Dataset 2	0.8275	0.8260	8.4987
	Dataset 3	0.8855	0.8943	7.0847
	Dataset 4	0.7883	0.8159	9.5607
	Dataset 5	0.8194	0.8234	9.6114
	Average	0.8268	0.8374	8.7495
BIQI [40]		0.8195	0.8205	15.6223
BLIINDS [41]		0.7996	N/A	N/A
PSNR		0.8197	0.8229	9.0929
SS-SSIM		0.8510	0.8636	8.1253

TABLE III
SROCC BETWEEN ALGORITHM AND DMOS

Method		JP2K	JPEG	WN	Blur	FF
GRNN	Dataset1	0.7760	0.9058	0.9813	0.8216	0.7504
	Dataset2	0.7356	0.8504	0.9782	0.8736	0.7753
	Dataset3	0.8649	0.8847	0.9786	0.8861	0.7900
	Dataset4	0.8078	0.8882	0.9795	0.6872	0.6921
	Dataset5	0.8937	0.8315	0.9792	0.8969	0.6692
	Average	0.8156	0.8721	0.9794	0.8331	0.7354
BIQI [40]		0.7995	0.8914	0.9510	0.8463	0.7067
PSNR		0.8898	0.8409	0.9853	0.7816	0.8903
SS-SSIM		0.9317	0.9028	0.9629	0.8942	0.9411

TABLE IV
LCC BETWEEN ALGORITHM AND DMOS

Method		JP2K	JPEG	WN	Blur	FF
GRNN	Dataset 1	0.8163	0.9007	0.9891	0.8278	0.7732
	Dataset 2	0.7251	0.8510	0.9885	0.8767	0.7925
	Dataset 3	0.8439	0.9277	0.9886	0.9205	0.8533
	Dataset 4	0.8052	0.9051	0.9887	0.6937	0.9387
	Dataset 5	0.9474	0.8145	0.9884	0.8062	0.7369
	Average	0.8276	0.8798	0.9887	0.8250	0.8189
BIQI [40]		0.8086	0.9011	0.9538	0.8293	0.7328
PSNR		0.8878	0.8596	0.9813	0.7840	0.8752
SSIM		0.9368	0.9297	0.9793	0.8741	0.9452

TABLE V
SROCC BETWEEN ALGORITHM AND DMOS BY INPUT FEATURE

Used feature	EPC +EDIS +MGDIS	MPC +EDIS +MGDIS	MPC +EPC +MGDIS	MPC +EPC +EDIS
SROCC	0.7372	0.8200	0.7523	0.7449

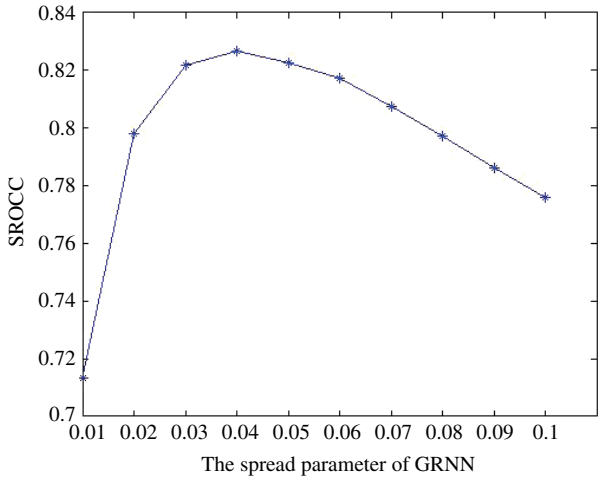

Fig. 4. Plot of SROCC against spread parameter.

In order to make the comparisons, we also plot the SROCC achieved by the new algorithm as the spread parameter is allowed to vary (Fig. 4).

From Table II, it can be seen that the GRNN-based algorithm outperforms the BIQI and BLIINDS indices and the FR index PSNR, although is a little inferior to the widely used FR index SS-SSIM. This is a remarkable result for an NR algorithm.

In order to further verify the performance of the phase congruency/entropy/gradient GRNN-based IQA algorithm, we also tested the GRNN-based algorithm on each distortion type in the LIVE IQA Database. Using the above trained GRNN-based IQA model, image quality is predicted on each distortion type yielding the results shown in Tables III and IV using 5-fold cross-validation.

Again, from these results, it can be seen that the GRNN-based algorithm outperforms the NR index BIQI, outperforms the FR index PSNR on the LIVE JPEG and Blur (sub) databases, and also performs well relative to SS-SSIM on the LIVE WN Database.

B. Perceptual Feature Analysis

In order to study the respective contributions of each feature that contributes to the overall quality score in the GRNN-based algorithm, we remove one input feature in turn, and then use the other three features to train and test the GRNN-based QA network by the above method, and yield the SROCC between the quality score and DMOS shown in Table V. A smaller value of the SROCC implies a bigger contribution from the removed feature. In this way, we can order the contributions

of the four input features in descending: MPC, MGDIS, EDIS, EPC. Since the EPC feature has little contribution to QA, we can ignore the EPC feature in actual application.

V. Conclusion

We developed a NR image quality prediction model based on several complementary and perceptually relevant image features fed to a GRNN network. The relationship between the extracted features and DMOS is modeled by the GRNN network. We found that the resulting image quality index produces results on the LIVE Image Quality Database that are generally comparable with competitive FR QA algorithms.

Looking forward, we are seeking to better characterize the functional relationship that exists between the perceptual feature set that we deployed, and recorded subjective scores. We are also investigating methods for efficiently extending the GRNN-based framework to *video* QA. Impairments are more complex and motion-related in video, making this a more challenging exercise.

Acknowledgment

The authors would like to thank those anonymous reviewers for their helpful comments.

References

[1] H. R. Sheikh, M. F. Sabir, and A. C. Bovik, "A statistical evaluation of recent full reference image quality assessment algorithms," *IEEE Trans. Image Process.*, vol. 15, no. 11, pp. 3441–3451, Nov. 2006.

[2] Z. Wang, E. P. Simoncelli, and A. C. Bovik, "Multiscale structural similarity for image quality assessment," in *Proc. 37th IEEE Asil. Conf. Signals, Syst. Comput.*, vol. 2. Pacific Grove, CA, Nov. 2003, pp. 1398–1402.

[3] Z. Wang and A. C. Bovik, "A universal image quality index," *IEEE Signal Process. Lett.*, vol. 9, no. 3, pp. 81–84, Mar. 2002.

[4] A. M. Eskicioglu and P. S. Fisher, "Image quality measures and their performance," *IEEE Trans. Commun.*, vol. 43, no. 12, pp. 2959–2965, Dec. 1995.

[5] S. A. Karunasekera and N. G. Kingsbury, "A distortion measure for blocking artifacts in images based on human visual sensitivity," *IEEE Trans. Image Process.*, vol. 4, no. 6, pp. 713–724, Jun. 1995.

[6] N. Nill, "A visual model weighted cosine transform for image compression and quality assessment," *IEEE Trans. Commun.*, vol. 33, no. 6, pp. 551–557, Jun. 1985.

[7] J. A. Saghri, P. S. Cheatham, and A. Habibi, "Image quality measure based on a human visual system model," *Opt. Eng.*, vol. 28, no. 7, pp. 813–818, Jul. 1989.

[8] Z. Wang, A. C. Bovik, H. R. Sheikh, and E. P. Simoncelli, "Image quality assessment: From error visibility to structural similarity," *IEEE Trans. Image Process.*, vol. 13, no. 4, pp. 600–612, Apr. 2004.

[9] C. Li and A. C. Bovik, "Three-component weighted structural similarity index," *Proc. SPIE-IS&T Electron. Imag.*, vol. 7242, pp. 72420Q-1–72420Q-9, Jan. 2009.

[10] H. R. Sheikh, A. C. Bovik, and G. de Veciana, "An information fidelity criterion for image quality assessment using natural scene statistics," *IEEE Trans. Image Process.*, vol. 14, no. 12, pp. 2117–2128, Dec. 2005.

[11] D. M. Chandler and S. S. Hemami, "VSNR: A wavelet-based visual signal-to-noise ratio for natural images," *IEEE Trans. Image Process.*, vol. 16, no. 9, pp. 2284–2298, Sep. 2007.

[12] B. Girod, "What's wrong with mean-squared error?" in *Digital Images and Human Vision*, A. B. Watson, Ed. Cambridge, MA: MIT Press, 1993, pp. 207–220.

[13] Z. Wang, A. C. Bovik, and L. Lu, "Why is image quality assessment so difficult?" in *Proc. IEEE Int. Conf. Acoust., Speech Signal Process.*, vol. 4. Orlando, FL, May 2002, pp. 1–4.

[14] M. P. Eckert and A. P. Bradley, "Perceptual quality metrics applied to still image compression," *Signal Process.*, vol. 70, no. 3, pp. 177–200, Nov. 1998.

[15] Z. Wang and A. C. Bovik, "Mean squared error: Love it or leave it? A new look at signal fidelity measures," *IEEE Signal Process. Mag.*, vol. 26, no. 1, pp. 98–117, Jan. 2009.

[16] *VQEG: The Video Quality Experts Group* [Online]. Available: http://www.vqeg.org/

[17] Z. Wang, G. Wu, H. R. Sheikh, E. P. Simoncelli, E.-H. Yang, and A. C. Bovik, "Quality-aware images," *IEEE Trans. Image Process.*, vol. 15, no. 6, pp. 1680–1689, Jun. 2006.

[18] H.-J. Park and H.-Y. Jung, "Reduced-reference quality assessment for JPEG-2000 compressed image," *IEICE Trans. Commun.*, vol. E91.B, no. 5, pp. 1287–1294, 2008.

[19] Z. Wang and E. P. Simoncelli, "Reduced-reference image quality assessment using a wavelet-domain natural image statistic model," *Proc. SPIE Human Vis. Electron. Imag.*, vol. 5666, pp. 149–159, Jan. 2005.

[20] H. R. Sheikh, A. C. Bovik, and L. Cormack, "No-reference quality assessment using natural scene statistics: JPEG2000," *IEEE Trans. Image Process.*, vol. 14, no. 11, pp. 1918–1927, Nov. 2005.

[21] Z. M. P. Sazzad, Y. Kawayoke, and Y. Horita, "No reference image quality assessment for JPEG2000 based on spatial features," *Image Commun.*, vol. 23, no. 4, pp. 257–268, Apr. 2008.

[22] Z. Wang, H. R. Sheikh, and A. C. Bovik, "No-reference perceptual quality assessment of JPEG compressed images," in *Proc. IEEE Int. Conf. Image Process.*, vol. 1. Rochester, NY, 2002, pp. I-477–I-480.

[23] P. Marziliano, F. Dufaux, S. Winkler, and T. Ebrahimi, "Perceptual blur and ringing metrics: Application to JPEG2000," *Signal Process.: Image Commun.*, vol. 19, no. 2, pp. 163–172, Feb. 2004.

[24] T. Brandão and M. P. Queluz, "No-reference image quality assessment based on DCT domain statistics," *Signal Process.*, vol. 88, no. 4, pp. 822–833, Apr. 2008.

[25] Z. Wang, A. C. Bovik, and B. L. Evans, "Blind measurement of blocking artifacts in images," in *Proc. IEEE Int. Conf. Image Process.*, vol. 3. Vancouver, BC, Canada, Sep. 2000, pp. 981–984.

[26] T. Vlachos, "Detection of blocking artifacts in compressed video," *Electron. Lett.*, vol. 36, no. 13, pp. 1106–1108, Jun. 2000.

[27] H. R. Wu and M. Yuen, "A generalized block-edge impairment metric for video coding," *IEEE Signal Process. Lett.*, vol. 4, no. 11, pp. 317–320, Nov. 1997.

[28] A. C. Bovik and S. Liu, "DCT-domain blind measurement of blocking artifacts in DCT-coded images," in *Proc. IEEE Int. Conf. Acoust., Speech, Signal Process.*, vol. 3. Salt Lake City, UT, May 2001, pp. 1725–1728.

[29] D. S. Turaga, Y. Chen, and J. Caviedes, "No reference PSNR estimation for compressed pictures," *Signal Process.: Image Commun.*, vol. 19, no. 2, pp. 173–184, Feb. 2004.

[30] J. Choe and C. Lee, "Estimation of the peak signal-to-noise ratio for compressed video based on generalized Gaussian modeling," *Opt. Eng.*, vol. 46, no. 10, pp. 107401-1–107401-9, Oct. 2007.

[31] A. Eden, "No-reference estimation of the coding PSNR for H.264-coded sequences," *IEEE Trans. Cons. Electron.*, vol. 53, no. 2, pp. 667–674, May 2007.

[32] A. Ichigaya, M. Kurozumi, H. Naohiro, Y. Nishida, and E. Nakasu, "A method of estimating coding PSNR using quantized DCT coefficients," *IEEE Trans. Circuits Syst. Video Technol.*, vol. 16, no. 2, pp. 251–259, Feb. 2006.

[33] D. S. Turaga, Y. Chen, and J. E. Caviedes, "No reference PSNR estimation for compressed pictures," in *Proc. IEEE Int. Conf. Image Process.*, vol. 3. Rochester, NY, Sep. 2002, pp. 61–64.

[34] A. Ichigaya, Y. Nishida, and E. Nakasu, "Nonreference method for estimating PSNR of MPEG-2 coded video by using DCT coefficients and picture energy," *IEEE Trans. Circuits Syst. Video Technol.*, vol. 18, no. 6, pp. 817–826, Jun. 2008.

[35] K. Nishikawa, K. Munadi, and H. Kiya, "No-reference PSNR estimation for quality monitoring of motion JPEG2000 video over lossy packet networks," *IEEE Trans. Multimedia*, vol. 10, no. 4, pp. 637–645, Jun. 2008.

[36] P. Gastaldo and R. Zunino, "Neural networks for the no-reference assessment of perceived quality," *J. Electron. Imag.*, vol. 14, no. 3, pp. 1–11, Aug. 2005.

[37] P. Gastaldo, R. Zunino, I. Heynderickx, and E. Vicario, "Objective quality assessment of displayed images by using neural networks," *Signal Process.: Image Commun.*, vol. 20, no. 7, pp. 643–661, Aug. 2005.

[38] R. V. Babu, S. Suresh, and A. Perkis, "No-reference JPEG-image quality assessment using GAP-RBF," *Signal Process.*, vol. 87, no. 6, pp. 1493–1503, Jun. 2007.
[39] A. Chetouani, A. Beghdadi, S. Chen, and G. Mostafaoui, "A novel free reference image quality metric using neural network approach," in *Proc. Int. Workshop Video Process. Qual. Metrics Cons. Electron.*, Scottsdale, AZ, Jan. 2010, pp. 1–4.
[40] M. Narwaria and W. Lin, "Objective image quality assessment based on support vector regression," *IEEE Trans. Neural Netw.*, vol. 21, no. 3, pp. 515–519, Mar. 2010.
[41] A. K. Moorthy and A. C. Bovik, "A two-step framework for constructing blind image quality indices," *IEEE Signal Process. Lett.*, vol. 17, no. 5, pp. 513–516, May 2010.
[42] M. A. Saad, A. C. Bovik, and C. Charrier, "A DCT statistics-based blind image quality index," *IEEE Signal Process. Lett.*, vol. 17, no. 6, pp. 583–586, Jun. 2010.
[43] T. Huang, J. Burnett, and A. Deczky, "The importance of phase in image processing filters," *IEEE Trans. Acoust., Speech, Signal Process.*, vol. 23, no. 6, pp. 529–542, Dec. 1975.
[44] A. V. Oppenheim and J. S. Lim, "The importance of phase in signals," *Proc. IEEE*, vol. 69, no. 5, pp. 529–541, May 1981.
[45] M. C. Morrone and R. A. Owens, "Feature detection from local energy," *Pattern Recognit. Lett.*, vol. 6, no. 5, pp. 303–313, Dec. 1987.
[46] S. Venkatesh and R. A. Owens, "An energy feature detection scheme," in *Proc. IEEE Int. Conf. Image Process.*, Singapore, Sep. 1989, pp. 553–557.
[47] P. Kovesi, "Image features from phase congruency," *J. Comput. Vis. Res.*, vol. 1, no. 3, pp. 1–26, 1999.
[48] M. C. Morrone and D. C. Burr, "Feature detection in human vision: A phase-dependent energy model," *Proc. Royal Soc. London B, Biol. Sci.*, vol. 235, no. 1280, pp. 221–245, Dec. 1988.
[49] B. Y. K. Aw, R. A. Owens, and J. Ross, "Image compression and reconstruction using a 1-D feature catalogue," in *Proc. Eur. Conf. Comput. Vis.*, Santa Margherita Ligure, Italy, May 1992, pp. 749–753.
[50] Z. Xiao, Z. Hou, C. Miao, and J. Wang, "Using phase information for symmetry detection," *Pattern Recognit. Lett.*, vol. 26, no. 13, pp. 1985–1994, Oct. 2005.
[51] M. J. Kyan, G. Ling, M. R. Arnison, and C. J. Cogswell, "Feature extraction of chromosomes from 3-D confocal microscope images," *IEEE Trans. Biomed. Eng.*, vol. 48, no. 11, pp. 1306–1318, Nov. 2001.
[52] N. Molton, X. Pan, M. Brady, A. K. Bowman, C. Crowther, and R. Tomlin, "Visual enhancement of incised text," *Pattern Recognit.*, vol. 36, no. 4, pp. 1031–1043, Apr. 2003.
[53] X.-B. Pan, M. Brady, A. K. Bowman, C. Crowther, and R. S. O. Tomlin, "Enhancement and feature extraction for images of incised and ink texts," *Image Vis. Comput.*, vol. 22, no. 6, pp. 443–451, Jun. 2004.
[54] Y. Huang, S. Lin, S. Z. Li, and H.-Y. Shum, "Face alignment under variable illumination," in *Proc. IEEE Int. Conf. Autom. Face Gesture Recognit.*, Seoul, Korea, May 2004, pp. 85–90.
[55] E. Bezalel and U. Efron, "Efficient face recognition method using a combined phase congruency/Gabor wavelet technique," *Proc. SPIE, Int. Soc. Opt. Eng.*, vol. 5908, pp. 59081K-1–59081K-8, Aug. 2005.
[56] Z. Xiao and Z. Hou, "Phase based feature detector consistent with human visual system characteristics," *Pattern Recognit. Lett.*, vol. 25, no. 10, pp. 1115–1121, Jul. 2004.
[57] P. Kovesi, "Phase congruency detects corners and edges," in *Proc. Australian Pattern Recognit. Soc. Conf.: DICTA*, Sydney, Australia, Dec. 2003, pp. 309–318.
[58] Z. Wang and E. P. Simoncelli, "Local phase coherence and the perception of blur," in *Proc. Adv. Neural Inf. Process. Syst.*, vol. 16. May 2004, pp. 1435–1442.
[59] Z. Liu and R. Laganiere, "Phase congruence measurement for image similarity assessment," *Pattern Recognit. Lett.*, vol. 28, no. 1, pp. 166–172, Jan. 2007.
[60] C. E. Shannon and W. Weaver, *The Mathematical Theory of Communication*. Urbana, IL: Univ. Illinois Press, 1949.
[61] E. N. Kirsanova and M. G. Sadovsky, "Entropy approach in the analysis of anisotropy of digital images," *Open Syst. Inf. Dyn.*, vol. 9, no. 3, pp. 239–250, 2002.
[62] S. Gabarda and G. Cristóbal, "Blind image quality assessment through anisotropy," *J. Opt. Soc. Amer. A*, vol. 24, no. 12, pp. B42–B51, Dec. 2007.
[63] D. F. Specht, "A general regression neural network," *IEEE Trans. Neural Netw.*, vol. 2, no. 6, pp. 568–576, Nov. 1991.
[64] S. Chartier, M. Boukadoum, and M. Amiri, "BAM learning of nonlinearly separable tasks by using an asymmetrical output function and reinforcement learning," *IEEE Trans. Neural Netw.*, vol. 20, no. 8, pp. 1281–1292, Aug. 2009.
[65] D. Tomandl and A. Schober, "A modified general regression neural network (MGRNN) with new, efficient training algorithms as a robust 'black box'-tool for data analysis," *Neural Netw.*, vol. 14, no. 8, pp. 1023–1034, Oct. 2001.
[66] Q. Li, Q. Meng, J. Cai, H. Yoshino, and A. Mochida, "Predicting hourly cooling load in the building: A comparison of support vector machine and different artificial neural networks," *Ener. Conv. Manage.*, vol. 50, no. 1, pp. 90–96, Jan. 2009.
[67] H. R. Sheikh, Z. Wang, L. K. Cormack, and A. C. Bovik. *LIVE Image Quality Assessment Database* [Online]. Available: http://live.ece.utexas.edu/research/quality
[68] *VQEG, Final Report from the Video Quality Experts Group on the Validation of Objective Models of Video Quality Assessment*. (2000, Mar.) [Online]. Available: http://www.vqeg.org/

Chaofeng Li author photograph and biography not available at the time of publication.

Alan Conrad Bovik author photograph and biography not available at the time of publication.

Xiaojun Wu author photograph and biography not available at the time of publication.